Surface modification of titanium dioxide nanotubes with sulfur for highly efficient photocatalytic performance under visible light irradiation

Ton Nu Quynh Trang[1], Le Thi Ngoc Tu[2], Co Le Thanh Tuyen[1], Tran Van Man[3], Vu Thi Hanh Thu[1],*

ABSTRACT

In this paper, the surface of titanium dioxide (TiO_2) nanotubes (NTs) was decorated with sulfur by impregnation procedure. The crystalline structure and morphology of the S-TiO_2 NT hybrid catalyst were investigated by X-ray diffraction (XRD) and transmission electron microscopy (TEM). The chemical components of S-TiO_2 NT-1 sample were analyzed by energy dispersive X-ray (EDX). The results showed that sulfur impurities were incorporated into TiO_2 crystal structure and decorated on its surface due to the heat treatment temperature used throughout the fabrication process. Moreover, its photocatalytic reaction was evaluated by change of adsorption intensity of methyl orange (MO) aqueous solution at wavelength of 467 nm. This work revealed that the sulfur loaded onto TiO_2 NT nanostructures exhibited excellent photocatalytic efficacy for the degradation of the MO dye compared with pristine TiO_2 NTs ($93.12 \pm 0.02\%$ and $80.21 \pm 0.04\%$ MO degradation efficacy under UV light versus visible-light regime, respectively, after 180 minutes). This was mainly governed by sulfur ions modified on the surface of TiO_2 NTs which played a critical role in promoting the separation rate of photo-induced charge carriers.

Key words: MO dye, Photocatalytic, Sulfur, TiO2 nanotubes, Visible light

[1]*Faculty of Physics and Engineering Physics, VNUHCM-University of Science, Viet Nam*

[2]*Faculty of Physics, Dong Thap University, Viet Nam*

[3]*Faculty of Chemistry, VNUHCM-University of Science, Viet Nam*

Correspondence

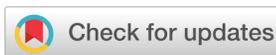**Vu Thi Hanh Thu**, Faculty of Physics and Engineering Physics, VNUHCM-University of Science, Viet Nam

Email: vththu@hcmus.edu.vn

Check for updates

VNU-HCM Press

INTRODUCTION

The energy crisis has drawn enormous attention in recent years due to an increasing demand for global energy and the rapid depletion of non-renewable energy resources[1,2]. Clean and renewable energy resources, such as solar energy, are not only the most abundant on earth but also without additional pollutant emission and economically viable, thus very crucial to the entire world. Among all these applications, photocatalysis has attracted much interest due to its great applications to solving environmental obstacles as a new approach for utilizing more effective solar radiation, since a pioneering report by Fujishima and Honda who demonstrated water splitting using titanium dioxide (TiO_2) in 1972[3]. Tremendous progress has been devoted to developing more efficient photocatalysts for water splitting under solar irradiation as one of the green and eco-friendly strategies to meet the energy needs of the world[4–7]. In addition to water splitting, photocatalysts exhibit a wide range of outstanding applications for disintegration of toxic organic pollutants, which has been useful in treating and purifying water and air.

Among all semiconductor types, titanium dioxide (TiO_2 is the most extensively investigated for photocatalysis, exhibits unique properties to meet the requirements of photocatalytic activity (due to its high stability during photoreactions), has superior redox ability, is nonhazardous, and is of low cost. However, the photocatalytic activity of TiO_2 has two major obstacles:

(**1**) TiO_2 (anatase) has a large band gap of 3.2 eV, and thus it can only act under UV light, which accounts for no more than 5% of total solar energy (thus a wide range of the solar energy would be wasted during the process and the desired applications of TiO_2 under sunlight would be significantly inhibited)[8]; and

(**2**) the rapid recombination of photogenerated electron-hole pairs. Hence, in order to address the aforementioned hindrances, numerous efforts can be employed for improving the photocatalysis and broadening the working regime to harness the visible light region.

Among all of the approaches, doping has been observed to be an effective method to increase the photocatalytic efficacy of TiO_2 under solar light[8–11], among which doping non-metal ions has been considered as one of the most promising approaches to reduce the TiO_2 bandgap because of suppression of the titanium d-states localization and its profound effects[12–14]. It is noteworthy that non-metal doped into the TiO_2 structure has been analyzed extensively, in

recent years, because the potential energy of O 2p atomic orbital is lower than the non-metal atomic orbital [15]. It may be speculated that in the case of anionic-doping, a new valence band is established instead of the O 2p atomic orbital; as a consequence, their bandgap energy is reduced [11,15,16].

Among these dopants, sulfur (S) doping has attracted considerable attention due to its highly thermal stability and remarkable improvement of visible light driven photocatalytic activity [17,18]. Ranjith *et al.* reported that sulfur-decorated TiO$_2$ nanowires synthesized by electrospinning process, to exhibit disintegration of RhB dye solution, was 4.8 times higher than pristine TiO$_2$ nanowires under visible regime [10]. Also, the high photocatalytic activity for the degradation of phenol compounds under UV light and solar light irradiation of S doped TiO$_2$ photocatalyst was attributed to the synergistic effects between sulfur ions with the modified surface, as studied by Devi *et al.* [19]. Moreover, Pham Van Viet *et al.* showed that Ag modified TiO$_2$ nanotube catalysts exhibited excellent degradation efficiency of methylene blue molecules under sunlight irradiation, due to the interaction between TiO$_2$ and Ag that promote the efficiency of photogenerated electron-hole pairs [20].

Based on the above findings, it may be proposed that TiO$_2$ amalgamated with sulfur plays a vital role in enhancing the disintegration of toxic organic pollutants under the regime of visible light and UV light. Therefore, in this research study, we prepared the doping of anatase TiO$_2$ with sulfur as a means to reduce their energy bandgap and obtain a red-shift on adsorption via the hydrothermal method and single-step reaction.

METHODS

Materials

The reagents in this study included titanium dioxide commercial powder (TiO$_2$, P25, 99.9%), sodium hydroxide pellets (NaOH, 99%), thiourea (>99%), and methyl orange (MO). All chemicals were purchased from Merck, Germany and used as received without any further purification. Double distilled water was used throughout the experiments, and all aqueous solutions were obtained from the Applied Physical Chemistry Laboratory of VNUHCM-University of Science.

Preparation

Synthesis of TiO$_2$ Nanotubes (NTs)

TiO$_2$ NTs have been successfully achieved through the hydrothermal method as described in our literature [21]. The schematic for the fabrication of TiO$_2$ NTs

is described in **Figure 1.**

Firstly, to prepare the precursor solution, 4.23 g TiO$_2$ powder was added to 120 mL of 10 mol/L of NaOH aqueous solution and stirred for 4 h at 50 °C. Secondly, the suspension was heated at 130 °C for 22 h in a closed Teflon-lined autoclave (190 mL). After that, the precipitates were collected by centrifugation, and the white product washed with double distilled water until pH 9.0 was achieved. Thirdly, the product was immersed in 2.0 M HNO$_3$ solution, and washed with double distilled water until pH 7.0. Finally, the sample was dried at 80 °C in an oven for 4 h and annealed at 400 °C for 2 h with a heating rate of 5 °C/min.

Synthesis of S co-catalyzed TiO$_2$ Nanotubes

TiO$_2$ catalyst decorated with sulfur was prepared by impregnation method. TiO$_2$ NTs were dispersed into sulfur solution (50 mL, the various wt % of S in the solution were 0.02, 0.04, and 0.06) in a glass beaker (100 mL) and stirred for 6 h at 80 °C. The product was air dried at 100 °C overnight, or until the water was completely evaporated and fine powder was obtained. These samples were annealed at 300 °C with a heating rate of 5 °C/min for 2 h to obtain the photocatalysts. They were marked as S-TiO$_2$ NTs-1, S-TiO$_2$ NTs-2, and S-TiO$_2$ and NTs-3, respectively.

Characterization

The crystalline phase of the photocatalyst was evaluated by a Bruker D8 ADVANCE X-ray diffractometer (XRD) with =0.15406 nm. The Diffuse Reflectance UV–visible spectra were measured on a UV-vis spectrophotometer (JASCO — V670) at the wavelength range of 300 – 700 nm, with a scan rate of 400 nm/min. The chemical component of S-TiO$_2$ NTs-1 sample were analyzed by energy dispersive X-ray (EDX). The morphology of the photocatalyst samples was characterized by scanning electron microscopy (SEM, Hitachi S-*4800)* equipped with an energy dispersive X-ray spectrometer (EDX), and transmission electron microscopy (TEM; JEM−1400) operated at 100 kV.

The photocatalytic activity of all the samples were explored by scrutinizing the disintegration of organic dyes (10 mg/L methyl blue) under UV light and visible irradiation, which was obtained from 25 W lamp (Reptile UVB100 — PT 2187), and 25 W lamp (a Philips visible light lamp, l>400 nm), respectively. Before visible light irradiation, control experiments were placed for 30 min in the dark to establish an equilibrium adsorption state. The degradation of MO dye was monitored by measuring their absorbance as a
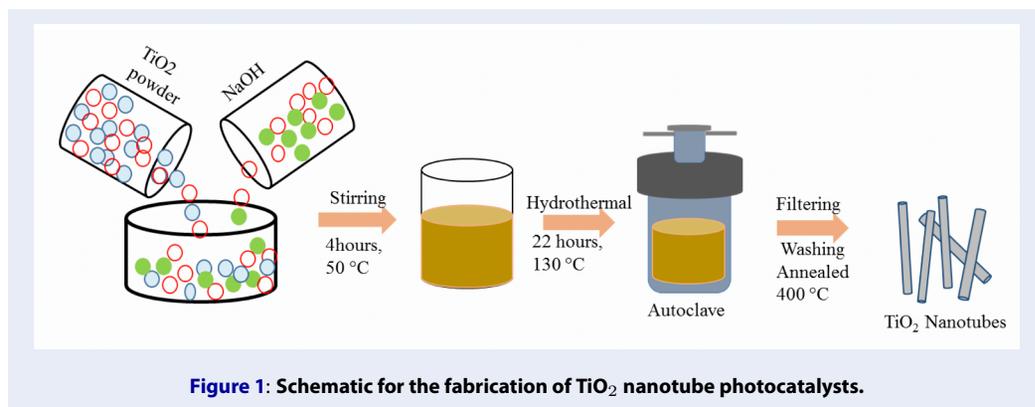
Figure 1: **Schematic for the fabrication of TiO$_2$ nanotube photocatalysts.**

function of irradiation time at predetermined time intervals using a UV-vis spectrophotometer (JASCO-V670) at 462 nm. The degradation efficiency of MO (C%) dye was determined by the following equation:

Degradation efficiency (%) = [(C$_0$ – C)/ C$_0$] x 100

where C$_o$ is the initial absorbance of MO, C is the absorbance of MO after reacting.

RESULTS

The morphology and structure of the pristine TiO$_2$ NTs and S-TiO$_2$ NTs were characterized by TEM, as presented in Fig. 2. The TiO$_2$ NT photocatalysts exhibited nanotube shape with a hollow center and opening at both ends (**Figure 2a**). The outer diameters of the nanotubes were between 10 and 11 nm, while the inner diameters were found to be approximately 4 nm. **Figure 2b** shows the TEM images of NT samples achieved by modifying the sulfidation precursor. The results revealed that compared to the pristine TiO$_2$ NTs, there was no significant surface morphological change over the sulfidation of NTs. Furthermore, some well-shaped nanocrystals were also observed on the surface of the TiO$_2$ NTs via modifying the sulfidation precursor, which was mainly governed by the formation of Ti-S on the surface.

Moreover, in order to further confirm the existence of sulfur (S), TiO$_2$ NTs decorated with sulfur were evaluated via energy dispersive X-ray analysis (EDX), as shown in **Figure 3**. The EDX spectrum revealed the presence of Ti, O, and S were observed in the as-prepared samples. Multiple elements, including Ti, O, and S, were detected in the photocatalyst. Ti and O were from TiO$_2$ NTs. Na was also detected, which was attributed to its use in the growth process of NTs. Meanwhile, the presence of sulfur demonstrated that S was successfully anchored onto TiO$_2$ NT structures. The peak intensity was associated with the concentration level of the element in the TiO$_2$ NTs. Although

the doping concentration of sulfur was low, the peaks (as presented in the EDX image) were revealed to be uniformly decorated in the photocatalyst structure.

Next, for identification of the phase composition and for structure characterization of pristine versus sulfidated TiO$_2$ NTs, the NTs were thoroughly investigated by X-ray diffraction patterns; the results are shown in **Figure 4**. The results revealed that the diffraction peak appeared at 2q = 25°, 38°, 48°, 54°, 55°, and 63°, which were ascribed to the diffraction of the (101), (004), (200), (105), (211), and (204) crystal planes, respectively (JCPDS cards no. 21-1272). No peak corresponding to rutile phase composition was observed in the spectrum, indicating that modifying the sulfidation precursor on the surface of TiO$_2$ NTs did not profoundly affect the phase or structure of anatase TiO$_2$ crystallites. The XRD patterns were clearly observed and the intensity of crystallization was further enhanced by an increase of the sulfur concentration. The latter was related to the heat treatment temperature used during fabrication which can favorably facilitate the nucleation growth of the anatase crystal. Moreover, a slight shift of anatase diffraction peak was detected (101), when compared with pristine TiO$_2$ NT; this similar result was confirmed by Wu *et al.* [22]. It can be concluded that the structural characterization achieved from XRD patterns were in agreement with TEM images.

The UV-Visible absorption spectroscopy has been considered as one of the major analytical techniques for the optical properties of a sample. The characterization of absorption and the energy band gap was calculated by Kubelka-Munk equation (E$_g$ = 1240.l^{-1}) of TiO$_2$ NTs and S-TiO$_2$ NTs, with different TiO$_2$:S ratio, were clearlydelineated in **Figure 5** (**a, b**). It was observed that pure TiO$_2$ NTs unveil a sharp absorption edge in the UV region (**Figure 5a**), corresponding to the band gap of 3.2 eV (**Figure 5b**), which was
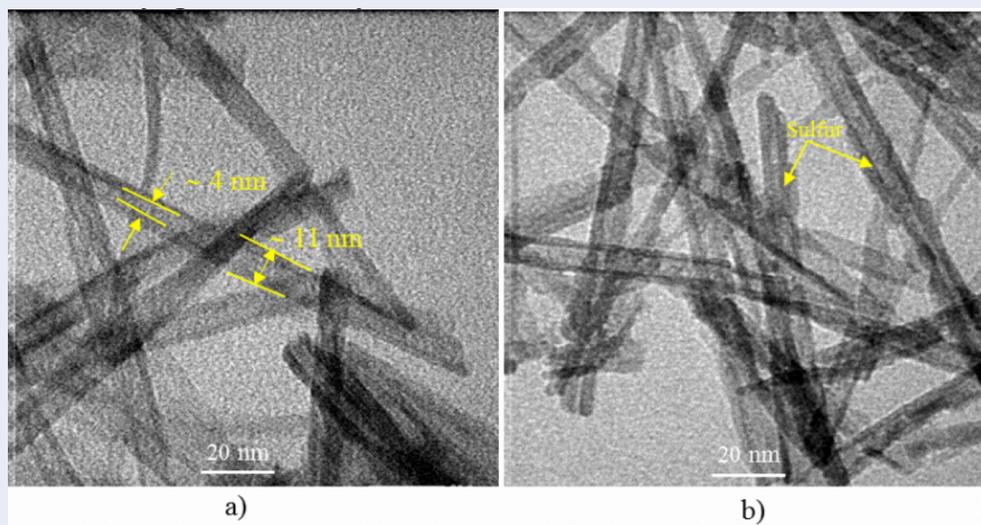
Figure 2: TEM images of (a) pristine TiO_2 NTs, or (b) as-prepared S-TiO_2NTs.
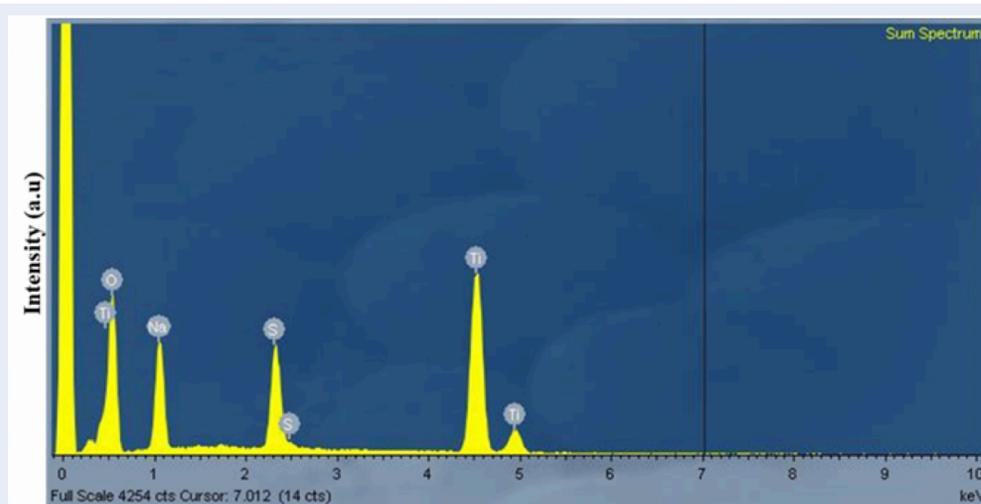

Figure 3: EDX elemental analysis of the as-prepared S-TiO_2 NT-1photocatalyst.

attributed to the transfer of valence band electrons to the conduction band. However, the S-TiO_2 NT photocatalysts exhibit a notable absorbance of the visible — light regime corresponding to the band gap of 2.8 eV (**Figure 5b**), which allows one to harness visible photons that could not be reached with one of the two materials alone. This can be explained by the formation of intermediate energy levels, which were created during the synthesis process. It may be speculated that these intermediate energy levels can significantly reduce the transition of electrons from the valence band to the conduction band, and causing the extension of the absorption edge in the visible light regime. As a result, a narrower band gap is achieved by modifying the TiO_2 with sulfur. Moreover, the rapid recombination rate of photogenerated charge carriers is significantly retarded via the interaction of S modified with TiO_2 NTs. These result in a markedly enhanced photocatalytic activity under visible-light regime. Hence, based on the above observations, it can be concluded that TiO_2 NTs, combined with sulfur, play a significant role in the disintegration of hazardous organic compounds in environmental remediation processes. Moreover, in order to further understand the relationship between sulfur and TiO_2 NTs, their photocatalytic behavior was investigated using MO as a probe
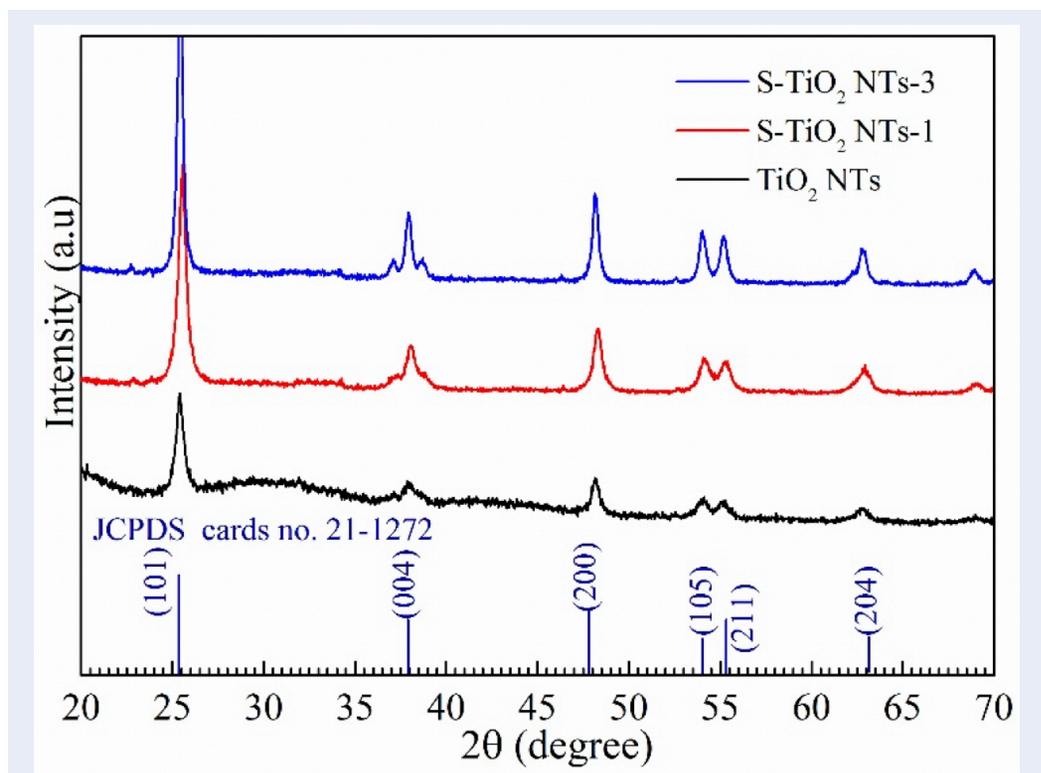
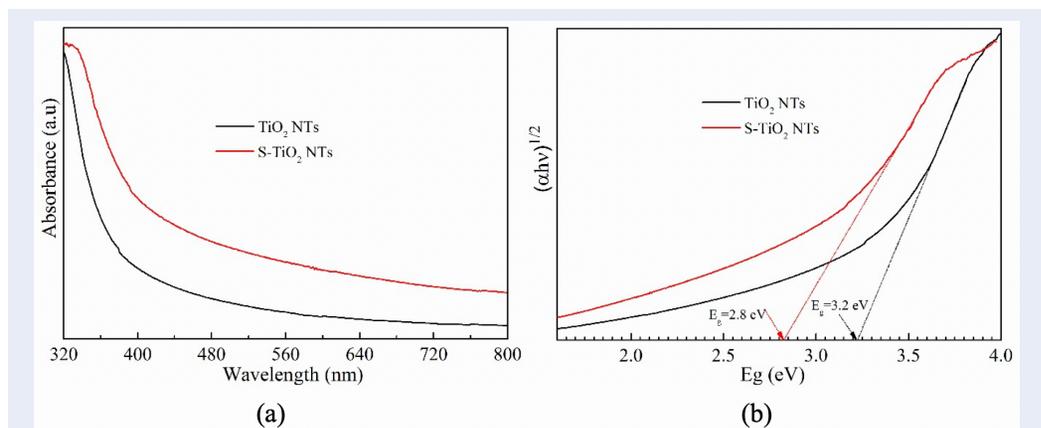**Figure 4**: XRD patterns of pristine TiO_2 NTs and as-prepared S-TiO_2 NTs.

(a)

(b)

Figure 5: The UV–Vis diffuse reflectance spectra (a) and plot of $(ahn)^{1/2}$ vs. photon energy (b) of pristine TiO_2 NTsand as-prepared S-TiO_2 NTs.

molecule with respect to time under UV and visible irradiation. The results are shown in **Figure 6**(**a, b**). **Figure 6**(**a,b**) reveals that no MO aqueous solution photodegradation was markedly observed when exposed to UV and visible-light regime irradiation, and without adding any photocatalyst. This could be attributed to that fact that photolysis does not occur in the degradation of MO under UV and visible light irradiation. While the degradation efficiency of MO molecules was significantly changed by the presence of the photocatalyst, it is well- justified. The presence of photocatalyst plays a critical role in enhancing the degradation performance. Additionally, as compared to pristine TiO$_2$ NTs, TiO$_2$ NTs decorated with sulfur exhibited a higher absorption rate under both UV light and visible light irradiation.

As shown in **Figure 6a**, the MO degradation efficacy was about 70.25 $\pm$ 0.02%, 78.60 $\pm$ 0.04%, 93.12 $\pm$ 0.02%, and 84.49 $\pm$ 0.04% for the pristine TiO$_2$ NTs, S-TiO$_2$ NT-1, S-TiO$_2$ NT-2, S-TiO$_2$ NT-3, respectively, under UV irradiation after about 180 min. The S-TiO$_2$ and NT-2 photocatalysts exhibit the best MO degradation performance. This can be explained by the electrostatic interaction of the sulfur impurities with the MO molecules, leading to the increased the number of surface's active sites and reduced rapid recombination of photogenerated electron-hole pairs. Moreover, the MO degradation activity of S-modified TiO$_2$ samples increases with increase of the S concentration and suddenly reduced for higher S levels. With increasing S concentration, the degradation efficacy was slightly decreased, which could be ascribed to the main factors: **i**) an excess of sulfur concentration (can act as a charge recombination center and reduce the efficient charge separation), and **ii**) higher S concentration; this complicates and may reduce the efficiency of the charge carriers[23].

Fig. 6b exhibits the MO degradation efficiency of pristine TiO$_2$ NTs and the surface-modified TiO$_2$ NTs with sulfur under visible light regime after 180 min. The results revealed that their degradation performance reached about 15.05 $\pm$ 0.03%, 77.03 $\pm$ 0.03%, 80.21 $\pm$ 0.04%, and 75.52 $\pm$ 0.03% for pristine TiO$_2$ NTs, S-TiO$_2$ NTs-1, S-TiO$_2$ NTs-2, S-TiO$_2$ NTs-3, respectively. The S-TiO$_2$ NT-2 sample exhibited the highest MO degradation efficiency. The main factors which affect the photocatalytic degradation efficiency of S-TiO$_2$ NT samples are similar to those affecting the results under UV light, as highlighted in **Figure 6a**. However, compared to **Figure 6a**, the MO degradation efficiency of a photocatalyst was lower under visible light (**Figure 6b**) than under UV light. This can be explained by the fact that pristine TiO$_2$

NTs are not activated under visible-light radiation and are not good candidates for visible light photocatalytic activity, leading to a slower reaction in the MO degradation process. On the other hand, doping sulfur into TiO$_2$ NTs, the photocatalyst may be activated under the visible light. As a consequence, the photogenerated electron-hole pairs take part in the redox reactions to disintegrate the MO aqueous solution; thus, the photocatalytic activity may be enhanced under the visible light irradiation.

Additionally, the apparent pseudo-first-order rate constants were determined through regression using a linearized, first order decay model ($-\ln(C/C_0) = kt$, where C_0 is the initial absorbance of MO, C is the absorbance of MO after reacting for a certain time t, and k is the rate constant portrayed in **Figure 6**(**c,d**). There is a highly linear correlation between $\ln(C/C_0)$ and the irradiation time (t), suggesting that the decomposition of the MO dye follows the first-order rate law under UV light and visible light, as shown in **Figure 6c** and **Figure 6d**, respectively. Under the visible light regime irradiation (**Figure 6d**), S-TiO$_2$ NT-2 exhibited the highest apparent rate constant of photocatalyst, which was estimated to be 0.0089 min^{-1}, and which is higher than that of TiO$_2$ NTs (0.0009 min^{-1}). Even under UV irradiation (**Figure 6c**), S-TiO$_2$ NT-2 had the highest reaction rate (0.015 min^{-1}), which is higher than the rate of TiO$_2$ NTs (0.0069 min^{-1}). It may be speculated that the promising photocatalytic degradation rate of S-TiO$_2$ NTs can be attributed to the improved carrier separation rate and reduced bandgap of the TiO$_2$, resulting in enhanced the absorption of visible light regime. It can be concluded that the degradation efficiency of the S-TiO$_2$ NTs samples for MO is in accordance with kinetic studies of photocatalytic degradation of the MO dye.

DISCUSSION

The MO degradation efficiency of sulfur-modified TiO$_2$ NTs improved remarkably compared with the pristine TiO$_2$ NTs under visible light irradiation. This demonstrated that sulfur was decorated successfully into the TiO$_2$ NT structure by impregnation method. It is, thus, desirable to explore the degradation mechanism of organic pollutants, which can be mainly ascribed to the generation of photoinduced reactive species through the separation of photogenerated charge carriers in the photocatalytic reaction system. When the photocatalyst is irradiated by an energy photon equal to or greater than the bandgap energy of the semiconductor, the photoinduced e$^-$
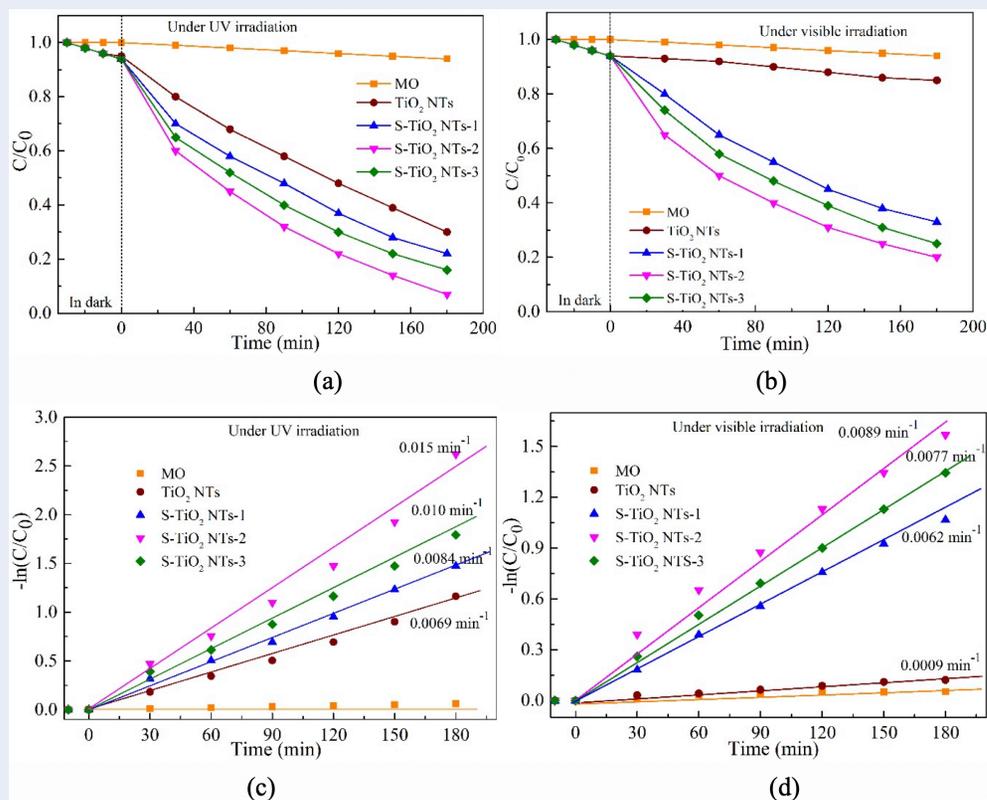
Figure 6: **Photodegradation performance and kinetics of MO photo degradation under UV (a, c) and visible light (c, d) for pristine TiO$_2$ NTs and S modified TiO$_2$ NT photocatalysts.**

— h$^+$ pairs are generated, the photogenerated electron accumulates on the surface of the photocatalyst near the junction, and rapidly reacts with adsorbed oxygen molecules to generate highly oxidative superoxide radical anions. On the other hand, photogenerated holes react with adsorbed H$_2$O or OH$^-$ group on the surface of a catalyst to produce a strong oxidizing agent. The overall highly active oxidation species mainly reacts with organic pollutant molecules. The major decomposition products of this process are released as CO$_2$, H$_2$O and inorganic ions. Thus, based on the above observations, it can be concluded that the sulfite-enhanced photocatalysis is an effective method to treat organic pollutants and anthropogenic wastewater, and may represent a new approach that plays a vital role in enhancing the mineralization of organic compounds under the visible-light regime. The sulfur loaded onto TiO$_2$ NTs structure is vital for designing the nanocomposite structure to disintegrate toxic organic pollutant; it has been considered as one of the most credible photocatalysts for organic dye degradation. Thus, the results of our research study showcase excellent MO degra-

dation efficacy at wavelength of 462 nm (of S-TiO$_2$ NTs not only under UV light but also under visible light irradiation). The results from this study provide rationale for the role of a photocatalyst in potential applications for environmental remediation practice.

CONCLUSIONS

In summary, in this study we have investigated the photocatalytic efficacy of TiO$_2$ NTs versus TiO$_2$ NTs modified with sulfur via hydrothermal treatment and impregnation method. The phase composition and structure characterization were not significantly changed after sulfur was modified onto TiO$_2$ NTs. Compared to the pure TiO$_2$ NTs, the absorption ability of S-TiO$_2$ NT samples improved remarkably in the visible light. Moreover, the prepared S-modified TiO$_2$ NTs exhibited a markedly enhanced visible light-driven photocatalytic activity for the disintegration of poisonous organic compounds. The degradation performance could reach up to 93.12 $\pm$ 0.02% and 80.21 $\pm$ 0.04% under UV light and visible light, respectively, after 180 minutes. This can be attributed to the improved efficiency of the separa-

tion of photogenerated electron-hole pairs and to the reduction of the energy bandgap of TiO2, which has been considered as the main reason for the enhanced photocatalytic activities under visible light regime. This data from this study provide a better understanding into the role of sulfur in designing a new strategic plan, such as one using efficient visible-light driven photocatalysts that can be developed more efficiently for future applications in the clinic.

COMPETING INTERESTS

The authors declare that there is no conflict of interest regarding the publication of this article.

AUTHORS' CONTRIBUTIONS

Ton Nu Quynh Trang has conceived of the present idea, carried out and written the manuscript with support from Vu Thi Hanh Thu

Le Thi Ngoc Tu and Co Le Thanh Tuyen carried out the experiments in group

Tran Van Man has supported the analysis techniques

ACKNOWLEDGMENTS

REFERENCES

1. Singh R, Dutta S. A review on H 2 production through photocatalytic reactions using TiO 2 /TiO 2 -assisted catalysts. Fuel. 2018;220:607–20. Available from: DOI:10.1016/j.fuel.2018.02.068.
2. Balzani V, Credi A, Venturi M. Photochemical conversion of solar energy. ChemSusChem. 2008;1:26–58. Available from: DOI:10.1002/cssc.200700087.
3. Fujishima A, Honda K. Electrochemical photolysis of water at a semiconductor electrode. Nature. 1972;238:37–8. Available from: DOI:10.1038/238037a0.
4. Zhang N, Zhang Y, Xu YJ. Recent progress on graphene-based photocatalysts: current status and future perspectives. Nanoscale. 2012;4:5792–813. Available from: DOI:10.1039/c2nr31480k.
5. Xie G, Zhang K, Guo B, Liu Q, Fang L, Gong JR. Graphene-based materials for hydrogen generation from light-driven water splitting. Advanced Materials. 2013;25:3820–39. Available from: DOI:10.1002/adma.201301207.
6. Abe R, Higashi M, Sayama K, Abe Y, Sugihara H. Photocatalytic activity of R3MO7 and R2Ti2O7 (R=Y, Gd, La; M=Nb, Ta) for water splitting into H2 and O2. The Journal of Physical Chemistry B. 2006;110:2219–26. Available from: DOI:10.1021/jp0552933.
7. Yerga RMN, Galvan MCA, del Valle F, de la Mano JAV, Fierro JL. Water splitting on semiconductor catalysts under visible-light irradiation. ChemSusChem. 2009;2:471–85. Available from: DOI:10.1002/cssc.200900018.
8. Asahi R, Morikawa T, Irie H, Ohwaki T. Nitrogen-doped titanium dioxide as visible-light-sensitive photocatalyst: designs, developments, and prospects. Chemical Reviews. 2014;114:9824–52. Available from: DOI:10.1021/cr5000738.
9. Liu G, Wang L, Yang HG, Cheng HM, Lu GQM. Titania-based photocatalysts—crystal growth, doping and heterostructuring. Journal of Materials Chemistry. 2010;20:831–843.
10. Ranjith KS, Uyar T. Rational synthesis of Na and S co-catalyst TiO 2 -based nanofibers: presence of surface-layered TiS 3 shell grains and sulfur-induced defects for efficient visible-light driven photocatalysis. Journal of Materials Chemistry A, Materials for Energy and Sustainability. 2017;5:14206–19. Available from: Doi:10.1039/c7ta02839c.
11. Peng Y, Ma Z, Hu J, Wu K. A first-principles study of anionic (S) and cationic (V/Nb) doped Sr 2 Ta 2 O 7 for visible light photocatalysis. RSC Advances. 2017;7:40922–40928.
12. Wang P, Wang J, Ming T, Wang X, Yu H, Yu J. Dye-sensitization-induced visible-light reduction of graphene oxide for the enhanced TiO2 photocatalytic performance. ACS Applied Materials & Interfaces. 2013;5:2924–9. Available from: DOI:10.1021/am4008566.
13. Pan L, Zou JJ, Wang S, Huang ZF, Zhang X, Wang L. - Enhancement of visible-light-induced photodegradation over hierarchical porous TiO2 by nonmetal doping and water-mediated dye sensitization. Applied Surface Science. 2013;268:252–8. Available from: DOI:10.1016/j.apsusc.2012.12.074.
14. Selvam K, Swaminathan M. Nano N-TiO 2 mediated selective photocatalytic synthesis of quinaldines from nitrobenzenes. RSC Advances. 2012;2:2848–2855.
15. Tang X, Li D. Sulfur-Doped Highly Ordered TiO 2 Nanotubular Arrays with Visible Light Response. The Journal of Physical Chemistry C. 2008;112:5405–9. Available from: DOI:10.1021/jp710468a.
16. Wu G, Nishikawa T, Ohtani B, Chen A. Synthesis and Characterization of Carbon-Doped TiO2 Nanostructures with Enhanced Visible Light Response. Chemistry of Materials. 2007;19:4530–7. Available from: DOI:10.1021/cm071244m.
17. Tian G, Pan K, Fu H, Jing L, Zhou W. Enhanced photocatalytic activity of S-doped TiO2-ZrO2 nanoparticles under visible-light irradiation. Journal of Hazardous Materials. 2009;166:939–44. Available from: DOI:10.1016/j.jhazmat.2008.11.090.
18. Naik B. Parida, K. M.; and Gopinath, C. S. - Facile synthesis of N-and S-incorporated nanocrystalline TiO2 and direct solar-light-driven photocatalytic activity. The Journal of Physical Chemistry C. 2010;114:19473–82. Available from: DOI:10.1021/jp1083345.
19. Devi LG, Kavitha R. Enhanced photocatalytic activity of sulfur doped TiO2 for the decomposition of phenol: A new insight into the bulk and surface modification. Materials Chemistry and Physics. 2014;143:1300–8. Available from: DOI:10.1016/j.matchemphys.2013.11.038.
20. Viet PV, Sang TT, Hien NQ, Thi CM. Synthesis of a silver/TiO 2 nanotube nanocomposite by gamma irradiation for enhanced photocatalytic activity under sunlight. Nuclear Instruments and Methods in Physics Research Section B: Beam Interactions with Materials and Atoms. 2018;429:14–18.
21. Le TN, Ton NQ, Tran VM, Nam ND, Vu TH. - TiO2 nanotubes with different Ag loading to enhance visible-light photocatalytic activity. Journal of Nanomaterials. 2017;2017:1–7. Available from: Doi:10.1155/2017/6092195.
22. Wu Q, Yang CC, van de Krol R. A dopant-mediated recombination mechanism in Fe-doped TiO2 nanoparticles for the photocatalytic decomposition of nitric oxide. Catalysis Today. 2014;225:96–101. Available from: DOI:10.1016/j.cattod.2013.09.026.
23. Ma D, Xin Y, Gao M, Wu J. Fabrication and photocatalytic properties of cationic and anionic S-doped TiO2 nanofibers by electrospinning. Applied Catalysis B: Environmental. 2014;147:49–57. Available from: DOI:10.1016/j.apcatb.2013.08.004.